Mol#31682

Title Page:

Chromanol 293B Binding in KCNQ1 (Kv7.1) Channels involves Electrostatic Interactions with a Potassium Ion in the Selectivity Filter

Christian Lerche, Iva Bruhova, Holger Lerche, Klaus Steinmeyer, Aguan D. Wei, Nathalie Strutz-Seebohm, Florian Lang, Andreas E. Busch, Boris S. Zhorov and Guiscard Seebohm

Physiology I, University of Tuebingen, Gmelinstr. 5, 72076 Tuebingen, Germany (C.L., K.S., N.S-S., F.L., A.E.B. G.S); Department of Biochemistry and Biomedical Sciences, McMaster University, 1200 Main Street West, Hamilton, Ontario, Canada L8N 3Z5 (I.B., B.S.Z.); Department of Neurology, University of Ulm, Oberer Eselsberg 45, 89081 Ulm, Germany (H.L.); Department of Anatomy and Neurobiology, Washington University School of Medicine, Saint Louis, MO 63110, USA (A.D.W.).

1

Mol#31682

Running Title Page:

Running Title:

Binding site of the chromanol 293B in KCNQ1 and I_{Ks} channels

Corresponding author:

Guiscard Seebohm

Physiology I, University of Tuebingen, Gmelinstr. 5, D-72076 Tuebingen, Germany

Tel.: +49 7071-29-78264, Fax.: +49 7071-29-3073,

email: guiscard.seebohm@gmx.de

Document statistics:

Text pages: 15 pages

Tables: 5

Figures: 5

References: 48

Abstract: 220 words

Introduction: 711 words

Discussion: 1278 words

List of nonstandard abbreviations:

293B, Chromanol 293B (trans-6-cyano-4-(N-ethylsulfonyl-N-methylamino)-3-hydroxy-2,2-dimethyl-chroman).

Abstract

The chromanol 293B (293B, trans-6-cyano-4-(N-ethylsulfonyl-N-methylamino)-3-hydroxy-2,2-dimethyl-chroman) is a lead compound of potential class III antiarrhythmics that inhibit cardiac I_{Ks} potassium channels. These channels are formed by the coassembly of KCNQ1 (Kv7.1, KvLQT1) and KCNE1 subunits. While homomeric KCNQ1 channels are the principal molecular targets, entry of KCNE1 to the channel complex enhances the chromanol block. Since closely related neuronal KCNQ2 potassium channels are insensitive to the drug, we used KCNQ1/KCNQ2 chimeras to identify the binding site of the inhibitor. We localized the putative drug receptor to the H5 selectivity filter and the S6 transmembrane segment. Single residues affecting 293B inhibition were subsequently identified through systematic exchange of amino acids either differing between KCNQ1 and KCNQ2, or predicted by a docking model of 293B in the open and closed conformation of KCNQ1. Mutant channel proteins T312S, I337V and F340Y displayed dramatically lowered sensitivity to chromanol block. The predicted drug binding receptor lies in the inner pore vestibule containing the lower part of the selectivity filter and the S6 transmembrane domain also reported to be important for binding of benzodiazepines. We propose that the block of the ion permeation pathway involves hydrophobic interactions with the S6 transmembrane residues I337 and F340, and stabilization of chromanol 293B binding through electrostatic interactions of its oxygens with the most internal potassium ion within the selectivity filter.

Introduction

KCNQ1 (Kv7.1, KvLQT1) channels are characterised by fast activation and delayed inactivation, but the coassembly with the accessory β-subunit KCNE1 (also named IsK or MinK, Takumi *et al*., 1988) results in slowly activating, non-inactivating potassium currents (Barhanin *et al.*, 1996; Sanguinetti *et al.*, 1996; Tristani-Firouzi and Sanguinetti, 1998). These heteromeric channels constitute the cardiac I_{Ks}-conductance, a component of the delayed rectifier repolarizing current I_K (Barhanin *et al.*, 1996; Sanguinetti *et al.*, 1996). Mutations in either gene can impair channel function and cause Long QT Syndrome (http://pc4.fsm.it:81/cardmoc/; Keating and Sanguinetti, 2001).

Most known class III antiarrhythmic drugs target I_{Kr}, the rapid component of the delayed rectifier I_K, which is encoded by the *HERG* gene and thereby cause prolongation of the cardiac action potential (Sanguinetti, 1992; Roden, 1993; Singh *et al.*, 1998). However, these medications possess a proarrhythmic potential and in turn may also increase the risk of life-threatening arrhythmias (Roden, 1993; Singh *et al.*, 1998). I_{Kr} blockade is also an undesirable side effect of systemic therapy by diverse antihistaminic, antibiotic, psychoactive and gastrointestinal prokinetic agents (http://www.torsades.org/medical-pros/drug-lists/drug-lists.htm). The molecular binding site in HERG was identified for a series of HERG blockers (Sanguinetti *et al*., 2005).

Alternatively, selective blockade of I_{Ks} (KCNQ1/KCNE1) has been suggested as a basis for more effective class III antiarrhythmic drugs (Sanguinetti and Jurkiewicz, 1991; Yang *et al.*, 2000; Gerlach, 2003). I_{Ks} is enhanced during β-adrenergic sympathetic stimulation, a known trigger of some forms of arrhythmias (Roden, 1993). Accordingly, prolongation of action potential duration by the selective I_{Ks} blocker chromanol 293B (293B) is greater after isoproterenol treatment (Schreieck *et al.*, 1997; Bosch *et al.*, 1998). Thus, chromanol 293B is a leading compound of a novel class of I_{Ks} blockers which share structural similarity with K_{ATP} channel openers (Gerlach *et al.*, 2001; Gerlach, 2003).

Determination of the binding sites of several K^+ channel blockers has increased our understanding of channel-drug interactions at the molecular level. Hanner *et al*. (2001) using binding studies, localized the correolide binding site in the central cavity of a 3D-homology model. Mitcheson *et al*. (2000) determined the putative binding site of HERG-blockers in the central cavity by Alanine-scanning combined with functional inhibition of channels by blockers. Subsequent studies on Kv1.5 blockers and our own work on KCNQ1 also localized inhibitor binding sites to the central cavity (Decher *et al.,* 2004; Seebohm *et al.*, 2003a), therefore suggesting that the central pore cavity of Kv-channels represents a preferential binding site for potent small molecule inhibitors conserved in different potassium channel families. In all these studies binding of the ligands to their receptors seem to depend mainly on hydrophobic and van der Waals interactions.

The recent definition of the binding sites of a blocking and a partially agonistic benzodiazepine (Seebohm *et al.*, 2003a; Seebohm *et al.*, 2003b) and the generation of a pharmacophore model (Du *et al.*, 2005) enhanced our knowledge of the molecular mechanisms involved in KCNQ1 channel block. This pharmacophore model suggested the importance of three hydrophobic and one central aromatic interactions. The hydrophobic regions within the pharmacophore are supposed to be about 9.1, 11.5, and 12.6 Å apart from each other. These distances are in good agreement with the putative high affinity binding mode of the benzodiazepine blocker L735821 (Seebohm *et al.*, 2003a), but do not satisfactorily explain the mode of binding of 293B, which is too small to fit the pharmacophoric points. The 293B molecule possesses a chroman scaffold to which an electron withdrawing cyano group is attached at the aromatic ring, which renders the molecule highly lipophilic, thereby favouring interactions with aromatic ring systems and hydrophobic side chains. Because 293B only contains this single hydrophobic area it does not exactly match the pharmacophoric features of the model proposed by Du *et al*. (2005).

To gain insight into the molecular requirements of 293B action, we pursued a combined domain transplantation and site-directed mutagenesis approach to test candidate positions in the pore region for participation in drug binding. By this, we identified the H5/S6 domain to be critical for drug sensitivity. Docking chromanol into closed and open conformations of KCNQ1 pore models based on the crystal structures of KcsA and Kv1.2 predicted binding of the ligand in the central cavity involving interactions with residues I337 and F340 and the most internal K^+ ion in the selectivity filter.

Materials and Methods

Molecular biology

Molecular biological procedures were performed as described previously (Seebohm *et al.*, 2001b). For chimera construction, silent mutations were introduced producing restriction endonuclease sites at corresponding positions in KCNQ1 and KCNQ2 flanking the region encoding the channel pore (SacI at amino acids "EL" 361/362, NsiI at amino acids "DAL" 301/302/303, and BamHI at amino acids "GS" 348/349 in KCNQ1). Other chimeric joining regions were created by recombinant PCR, resulting in constructs shown in Fig. 2. The megaprimer method was used for site-directed mutagenesis using cloned PfuI DNA polymerase (Promega GmbH, Mannheim, Germany). All constructs were verified by automated DNA sequencing. KCNQ cDNA constructs in pSGEM were linearized with NheI, and cRNA was synthesized by *in vitro* transcription (mMessage mMachine T7 kit, Ambion, Applied Biosystems, Darmstadt, Germany). CRNA concentrations were determined by photospectrometry and transcript quality was checked by agarose gel electrophoresis. Enzymes were purchased by NEB (New England Biolabs, MA, USA) if not otherwise stated. Sequences of cDNA clones were (human KCNQ1: XM_052604.2, human KCNQ2: AF110020, rat KCNQ3: NM_032597, human KCNQ4: NM_004700, human KCNQ5: NM_019842, human KCNE1: NM_000219, KQT1: AY572974).

Two-electrode voltage clamp technique (TEVC)

TEVC was performed as previously reported (Lerche *et al.*, 2000a; Seebohm *et al.*, 2001a). Briefly, *Xenopus laevis* ovaries were obtained from tricaine anesthetized animals. Oocytes were collagenase-treated (1 mg/ml, type II, Worthington, Lakewood, NJ, USA) in OR2 solution (NaCl 82.5 mM, KCl 2 mM, $MgCl_2$ 1 mM, HEPES 5 mM, pH 7.4) for 120 min and subsequently stored in recording solution ND96 (NaCl 96 mM, KCl 2 mM, $CaCl_2$ 1.8 mM, $MgCl_2$ 1 mM, HEPES 5 mM, pH 7.4) with additional sodium pyruvate (275 mg/l),

theophylline (90 mg/l) and gentamycin (50 mg/l) at 18°C. Each oocyte was injected with 10 ng cRNA encoding either WT or mutant KCNQ subunits, or coinjected with either WT or mutant KCNQ1 (10 ng) and KCNE1 (5 ng). Standard TEVC recordings were performed at 22°C with a Turbo Tec 10CX (NPI, Tamm, Germany) amplifier, an ITC-16 interface combined with Pulse software (Heka, Lambrecht/Pfalz, Germany) and Origin version 6.0 (Additive, Friedrichsdorf/Ts, Germany) for data acquisition. Macroscopic currents were recorded 3-4 days after injections. Pipettes were filled with 3 M KCl and had resistances of 0.5 – 1.5 MΩ. Proper voltage clamp was provided using the amplifiers integrator and visual control of the PI-controller. Chromanol 293B was synthetised by the Medicinal chemistry group of Aventis Pharma. Chromanol 293B-containing solutions were freshly prepared from a 100 mM DMSO stock solution. The maximal achievable 293B concentration was 100 µM. Chemicals were purchased from Sigma-Aldrich Chemie GmbH (Munich, Germany) if not stated otherwise. Student's t test was used to test for statistical significance, which was assumed at $p < 0.05$ (indicated by asterisk).

Molecular modeling

Molecular modeling was performed using the ZMM program (www.zmmsoft.com) which employs the Monte Carlo-minimization algorithm to search for optimal conformations (Li and Scheraga, 1987). Atom-atom interactions were calculated using the AMBER force field (Weiner *et al.*, 1984). The cut-off distance of 8 Å was used. Hydration energy was calculated using the implicit-solvent method (Lazaridis and Karplus, 1999). Ionizable residues of the protein were kept in the neutral form (Momany *et al.*, 1975; Lazaridis and Karplus, 1999).

The X-ray structures of KcsA (Doyle *et al.*, 1998) and Kv1.2 (Long *et al.*, 2005) served as templates for closed and open conformations of the KCNQ1 channel S5/H5/S6 domain, respectively. The alignment is shown in Table 4. The extracellular H5 loop residues

in KCNQ1 (amino acids 291-294), which are not present in KcsA and Kv1.2, were not modeled. These loops are too far from the ligand-binding site, and therefore, this approximation does not affect our results. During energy minimizations, the alpha carbons of the proteins were constrained to corresponding positions of the templates using pins. The pins are flat-bottom constraints, which allow penalty-free deviation up to 1 Å, and impose a penalty of 10 kcal mol^{-1} Å^{-1} for deviations > 1 Å. The binding sites of K^{+} ions in the selectivity filter are numbered from 1 to 4 starting from the extracellular side (Zhou and MacKinnon, 2003). Positions 2 and 4 were loaded with K^{+} ions, and positions 1 and 3 with water molecules.

Atomic charges in 3R,4S-chromanol 293B were calculated by the AM1 method using MOPAC. Bond angles of the ligand were allowed to vary in energy minimizations. The optimal positions and orientations of the ligand in the closed channel were initially searched by generating 20,000 random starting points with the mass center occurring within a cylinder of 16 Å in diameter and 13 Å in length. The axis of the cylinder coincided with the long axis of the pore. In the open channel, the corresponding cylinder was 20 x 18 Å. The area of the random search covered the entire pore region, including interfaces between domains. From each starting position, the energy was minimized in the absence of the solvent. The energy-minimized conformations within 100 kcal mol^{-1} from the apparent global minimum were further energy-minimized in water until the last 1000 energy minimizations did not improve the best minimum found.

Results

Closely related KCNQ potassium channels differ in their chromanol sensitivity

Different KCNQ channels were expressed in *Xenopus* oocytes and their sensitivity to chromanol 293B was determined using the two-electrode voltage clamp (TEVC) technique. Homomeric KCNQ1 channels were inhibited with an IC_{50} value of 26.9 ± 0.8 µM (Figures 1-3, Tables 1-3). Since heteromeric KCNQ1/KCNE1 subunits were more sensitive to 293B ($IC_{50} = 6.9 \pm 0.5$ µM, Figures 1B, 3, Tables 1, 3) than KCNQ1 channels alone, this drug may exert an I_{Ks} preference *in vivo*. KQT-1, the KCNQ1 homologue from *C. elegans* (Wei *et al.*, 2005), was also highly sensitive to 293B ($IC_{50} = 16.2 \pm 1.3$ µM, Figure 1H). Homomeric KCNQ5 currents were only moderately inhibited by 293B (Figure 1G), whereas homomeric KCNQ2, KCNQ3, KCNQ4, and heteromeric KCNQ2/KCNQ3 channels were only slightly blocked by 100 µM of 293B (Figure 1C-F, table 1).

Identification of regions in KCNQ1 responsible for chromanol 293B sensitivity

To elucidate the structural determinants of 293B sensitivity we studied a series of functional chimeras between chromanol-sensitive KCNQ1 and insensitive KCNQ2 channel subunits (Figure 2). Several of these chimeras were previously described and kinetically characterized (Seebohm et al., 2001b). Since C-terminal tails of KCNQ channels mediate subunit assembly (Schmitt et al., 2000; Maljevic et al., 2003; Schwake et al., 2003), they could be involved in drug inhibition mediated by disruption of the channel complex. However, a KCNQ1 protein with a KCNQ2 C-terminus (Q1tailQ2) still expressed currents with similar sensitivity to block by 293B as wild type KCNQ1 currents ($IC_{50} = 27.8 \pm 3.1$, n = 4, not shown), demonstrating that this area is not important for drug inhibition. The inverse chimera (Q2tailQ1) did not yield functional channels (not shown).

Since the pore region is preferentially targeted by several potassium channel blocking drugs (Mitcheson et al., 2000; Hanner et al., 2001; Seebohm et al., 2003a; Sanguinetti et al.,

2005), we exchanged the S5/H5/S6 region of KCNQ1 and KCNQ2, to create the Q1S5S6Q2 and Q2S5S6Q1 chimeras. Q1S5S6Q2 was almost insensitive to chromanol 293B (20 % block by 100 µM 293B; Figure 2A upper right, Table 2). On the other hand, 293B sensitivity could be transferred to KCNQ2 along with the S5/H5/S6 domain of KCNQ1 (Q2S5S6Q1; IC$_{50}$ value of 56 µM; Figure 2A upper right, Table 2). These results clearly identified the pore region as the critical determinant of 293B activity. To further narrow down the sites of 293B binding, we then exchanged smaller parts of the S5/H5/S6 domain. Substitution of the S5-H5 linker in KCNQ1 by the corresponding sequence of KCNQ2 (Q1S5linkerQ2, Figure 2A lower left) did not affect 293B sensitivity, although this region shows only low sequence similarity. Likewise, a KCNQ1 chimera containing S5 of KCNQ2 exhibited only slightly reduced 293B sensitivity (Q1S5Q2, Figure 2A lower left). In contrast, KCNQ1 channels with S5 through H5 of KCNQ2 were dramatically less sensitive to 293B (Q1S5H5Q2, 35 % block by 100 µM 293B; Figure 2A lower right), as was the case with KCNQ1 containing the H5-S6 linker and S6 segment of KCNQ2 (Q1H5S6Q2, less than 10 % block by 100 µM 293B; Figure 2A lower right). These results revealed that the H5 selectivity filter and S6 transmembrane segment are the principal determinants of 293B affinity in KCNQ1.

Point mutations of the KCNQ1 pore

Alignment of protein sequences spanning H5 and S6 regions of all KCNQ channels identified several residues present in KCNQ1 as potential interaction partners of the 293B molecule (e.g. residues 307, 308, 326, 327, 330, 331, and 337, marked by arrows in Fig. 2B). We constructed KCNQ1 channels with either single or double substitutions of the corresponding amino acids of KCNQ2, and tested for inhibition by 293B (Table 3). Double exchanges at positions 326/327 and 330/331 did not significantly relieve the 293B block. However, single point mutations V307L in the H5 pore helix and I337V in the S6

transmembrane helix significantly decreased the sensitivity to chromanol 293B (Figure 3A, C, Table 3).

As next, we introduced more conservative exchanges in the regions around residues V307 and I337. We found that conservative mutation T312S strongly reduced current inhibition (Figure 3G, Table 3), whereas the same mutation at the neighboring position, T311S, had no effect and that mutation V310L caused a 2.6-fold decrease in sensitivity to 293B block (Table 3). Mutations around position I337 generally decreased sensitivity to 293B and mutating the Phenylalanine at position 340, which is strictly conserved in all KCNQ channels, to a Tyrosine or Isoleucine caused the strongest reduction in 293B sensitivity (Figure 3, Table 3). In summary, the strongest effects on 293B block occurred by mutating a single residue (T312) in the lower selectivity filter and two residues in the central cavity, namely I337 and F340.

Introduction of Chromanol 293B sensitivity into KCNQ2

To corroborate our findings, we introduced the identified amino acids into the KCNQ2 channel (V307 and I337 in KCNQ1 correspond to L272 and V302 in KCNQ2, respectively, Figure 2B). In fact, these reciprocal substitutions (KCNQ2 L272V/V302I) increased 293B sensitivity seven-fold, as compared to wild-type KCNQ2 (34.7 ± 1.7% vs. 5.0 ± 1.0% inhibition at 100 µM, n = 3, Figure 4). These experiments confirmed the importance of these two residues for the sensitivity of KCNQ1 channels to 293B block.

KCNE1 effects on channel gating and 293B block can be functionally separated

Since KCNE1 in addition to slowing activation kinetics and increasing current amplitudes also increases 293B sensitivity of KCNQ1, we also investigated chromanol block of mutant KCNQ1 subunits in presence of KCNE1. With mutants V307L, I337V, and F340Y, activation kinetics were slowed after coexpression with KCNE1, similar as for wild-type

KCNQ1. Mutant T312S, which generates only small currents also did not show increased I_{Ks}-like currents, and therefore, we could not test 293B sensitivity of these mutant heteromeric channels. However, coexpressed KCNE1 while showing typical effects on current gating and amplitude did no longer augment the sensitivity to 293B of KCNQ1 mutants V307L and I337V (Figure 3A-D, Table 3). These findings indicate that modulatory effects of KCNE1 on chromanol 293B pharmacology and on activation kinetics of resulting I_{Ks} currents can be functionally separated.

Molecular modeling of the KCNQ1 chromanol 293B binding site

To further corroborate the results from our functional expression studies, we performed extensive molecular modeling. We used the X-ray coordinates of KcsA and Kv1.2 crystal structures to construct homology models of the closed and open KCNQ1 pore, respectively (based on the protein sequence alignment shown in Table 4), and subsequently docked 293B into the pore models. Since our previous work on state-dependent binding of chromanol suggested a preferential open channel block mechanism (Seebohm *et al.*, 2001a), we first investigated the open pore conformation. 20,000 orientations of the ligand were randomly sampled in the Kv1.2-based model of the open KCNQ1 channel pore (Figure 5A, B). Several ligand-receptor complexes were found with the ligand-receptor energy within 5 kcal/mol from the apparent global minimum (Figure 5C, D). In these energetically most favoured complexes, the largest stabilizing contribution to the binding of chromanol is provided by the K^+ ion in position 4. In some complexes, the K^+ ion interacts either with the SO_2 or OH group of the ligand. In the apparent global-minimum complex, both groups chelate the K^+ ion (Figure 5E, F) that provides -14.1 kcal/mol to the binding energy. In addition to the interaction with K^+, the ligand is stabilized by pore-facing residues I337 and F340 (Figure 5E, F; Table 5). In addition, chromanol also favorably interacts with T311 and T312 in the selectivity filter (Table 5). When summed over four domains, the energy of interactions of

13

chromanol with T312 was negative (attractive), but energy contributions of residues from individual domains varied between −2.2 and +1.9 kcal/mol (Table 5). The repulsion between T312 in two domains and chromanol is not a result of poor optimization, but is caused by a strong attraction of the ligand to K^+ in position 4.

Structure-activity relationships of chromanol analogs (Gerlach *et al.*, 2001) revealed that replacement of the cyano group by large bulky groups produces more active compounds, showing that it is not an indispensable determinant of chromanol activity. In our model, the cyano group faces either the cytoplasmic side or the interdomain space suggesting that its replacement with a larger alkyl group would increase van der Waals interactions without affecting the tertiary complex between the oxygen atoms of the drug, the K^+ ion in position 4, and residues of the channel..

The docking model strongly suggests, that interactions of 293B mainly take place with amino acids T312, I337 and F340 as well as an K^+ ion in the selectivity filter, indicating that observed changes in 293B blocking capability by mutation of other amino acids (amino acids 307, 335, 336, 338 and 339) rather occurred as an indirect result from induced structural changes of the potassium channel protein.

We next explored the possibility of chromanol binding to the KcsA-based model of the closed (resting) KCNQ1 channel. Again, after randomly sampling of 20,000 orientations of the ligand, the energetically most favorable binding mode of chromanol was found to be inside the water-lake cavity (Figure 5*G*, *H*). As in the open channel pore, the largest contributions to the ligand-receptor energy is provided by the K^+ ion in position 4 and residues I337 and F340 (Table 5). Despite the favorable (negative) ligand-receptor energy, the ligand experienced strains inside the inner cavity implying that the latter is too small to accommodate a bulky chromanol molecule. However, since the overall ligand-binding energy of chromanol is negative, we cannot completely rule out the possibility that the ligand can

14

bind inside the closed channel, though our combined results rather favour binding inside the

open channel.

Discussion

Pharmacological block of potassium channels can be accomplished by plugging the ion permeation pathway or by altering their gating. In case of gating modifiers the current through ion channels is reduced by stabilization of non-conduting closed or inactivated states. A pore plugging mechanism of 293B inhibition of KCNQ1 channels is strongly suggested by several experimental findings: Chromanol 293B can achieve an almost complete block in a voltage-independent fashion, and also does not markedly affect channel kinetics (Yang *et al.*, 2000; Seebohm *et al.*, 2001a). The 3R,4S enantiomer of 293B exhibited a weak state dependence, which indicated that it binds into the open channel (Seebohm *et al.*, 2001a).

The present investigation was performed to further the knowledge about the binding mode and blocking mechanism of 293B. Using a chimera and single point mutational approach we identify residues in the S6 transmembrane domain (I337, F340) and lower selectivity filter (T312) of the channel as crucial determinants of 293B sensitivity, strongly suggesting that the 293B receptor is located in the central pore cavity. To corroborate these experimental findings we performed homology modeling and unbiased docking of chromanol in the closed and open KCNQ1 channels by generating a large number of starting conformations and energy optimizing them. The obtained results confirm the mutagenesis data and propose that residues I337 and F340 essentially contribute to the ligand-receptor complex. Interestingly, nearby conservative exchanges F335Y, A336T, S338T and F339Y also caused a significant reduction of 293B sensitivity. However, we believe that these exchanges rather alter the sterical configuration of the neighbouring crucial residues I337 and F340, and/or hinder the access of 293B to the binding site. To corroborate this notion and the importance of the hydrophobic interactions with the cavity wall, we modeled the F340A mutant and then calculated the total energy of the ligand-receptor complex in this mutated channel. The obtained ligand-receptor energy of 293B was -17.8 kcal/mol, which indicates a significantly weaker binding as in the wild-type channel (-20.2 kcal/mol). Moreover, we

16

found that the K^+ ion in position 4 of the selectivity filter is a further major contributor to the ligand-receptor binding energy. This suggests the formation of a tertiary complex between 293B, the permeating K^+ ion, and residues facing the cavity of the channel. Ligand-receptor interaction may be stabilized by the two oxygens within the sulfonamide (N-ethylsulfonyl-N-methylamino) group and the oxygen attached to C3 of the chroman ring, that together generate a negatively charged surface (Figure 5I), and according to our docking model interact with the innermost potassium ion in the selectivity filter (K^+ at position 4). This prediction is further strengthened by the finding that substitution of the ethyl within the sulfonamide group by a bulkier substituent like butyl largely increases the IC_{50} value (Gerlach *et al.*, 2001). A bulkier substituent presumably would weaken the interaction of the oxygens with the selectivity filter potassium ion. Substitutions at the aromatic ring with bulky lipophilic side chains (higher alkoxy substituents such as butoxy) increased the activity of the chroman structures to IC_{50} values as low as 50 nM (substance 8a in Gerlach *et al.*, 2001), whereas substitution of the sulfonamide group with a pyrolidine ring eliminated the block of the resulting substance (Gerlach *et al.*, 2001). Both findings are consistent with our docking model. Finally, the sulfonyl group is attached to C4 and the oxygen to C3 of the chroman ring. C3 and C4 represent chiral centers and the 3R,4S-conformer shows a higher potency at opened channels in electrophysiological recordings. The relative position of the chroman ring to the three oxygens depends on the chirality and thereby may determine the mode of drug interaction with I337, F340 and the potassium ion and 293B pharmacology (Yang *et al.*, 2000; Seebohm *et al.*, 2001a). Other energetically less favoured binding modes of the small 293B molecule in the channel cannot be fully excluded but they would be less stable. The mode of drug interaction as proposed by the docking model implies that 293B inhibits KCNQ1 channel activity by a direct block of the ion permeation pathway.

The participation of conducting ions in the binding of ligands to the pore region was earlier proposed in molecular modeling studies of Ca^{2+} and Na^+ channels (Zhorov and

Ananthanarayanan, 1996; Zhorov *et al.*, 2001; Tikhonov and Zhorov, 2005; Wang *et al.*, 2006). Bruhova and Zhorov (2007) docked correolide inside the open homology pore of the Kv1.3 channel, and found that the K^+ ion in position 4 is an indispensable determinant of the correolide receptor. Correolide is much larger than chromanol 293B, but both drugs share common features that allow them to bind with high affinity to K^+ channels. These include the ellipsoid-like shape with nucleophilic groups at the poles and hydrophobic sides. The drugs can reach the K^+ ion bound to the cytoplasmic side of the selectivity filter by their polar groups while their hydrophobic sides engage hydrophobic interactions with the predominantly hydrophobic inner helices.

How exactly blocks 293B ion conduction? The hydrophobic and electrostatic interactions of 293B binding to the channel may ultimately disturb the coordination of the permeating potassium ions in the cavity and in the selectivity filter, that is of vital importance for ion conduction (Doyle *et al.*, 1998; Roux and MacKinnon, 1999; Zhou and MacKinnon, 2004a; Zhou and MacKinnon, 2004b). Consistently, mutations adversely affecting 293B block are located in close proximity to these sites in the cavity and base of the selectivity filter. In particular, the threonines at the base of the selectivity filter (T312 in KCNQ1) are involved in the formation of K^+-binding site 4. Furthermore, blocking activity of 3R,4S-293B mildly increased with extracellular potassium (IC_{50} at high extracellular K^+: 10 ± 2 μM, IC_{50} at low extracellular K^+: 16 ± 4 μM; Seebohm *et al.*, 2001a). The X-ray structure of the KcsA channel showed that K^+ ion concentration affects the equilibrium between distinct selectivity filter conformations (Zhou *et al.*, 2001). At low K^+ concentration (a few millimolar), the filter loses one of its dehydrated K^+ ions and undergoes structural changes, whereas at higher K^+ concentrations the filter adopts a conductive conformation and occupancy of K^+-binding site 4 may be increased (Zhou *et al.*, 2001). This site coordinates the potassium ion predicted to interact with the 293B-oxygens, and its increased occupancy thus in turn may stabilize 3R,4S-293B-binding. Electrostatic interactions of permeating potassium ions with pharmacological

18

reagents, as in case of the Kv channel blocker correolide (Bruhova and Zhorov, 2007), and as proposed here for 293B, may eventually be a frequent feature of K^+ channel blocker interactions.

The modulatory role of the KCNE1 β-subunit in the sensitivity of the KCNQ1 channel to 293B is still not very well understood. The fact that KCNE1 increases the sensitivity to 293B but simultaneously relieves current inactivation already argues against stabilization of the inactivated state of the channel by 293B. Moreover in the course of this work, we identified two KCNQ1 mutations, namely V307L and I337V, which eliminate the modulatory effect of KCNE1 on chromanol sensitivity, while retaining its effect on channel gating. One residue is located in the pore helix (V307) and the other in the inner cavity (I337). Since KCNE1 possibly binds to the outer face of S6 and S5 (Tapper and George Jr, 2000; Melman *et al.*, 2004) and is not directly involved in formation of the central cavity and the selectivity filter, this could indicate that it does not directly take part in chromanol binding but acts allosterically to facilitate drug binding to the principal KCNQ1 subunit (Lerche et al., 2000b). While our findings now suggest that facilitation of channel gating and 293B activity are independent actions of the accessory subunit, further studies are clearly necessary to elucidate the exact mechanisms of this modulatory interaction.

Mol#31682

Acknowledgements

20

References

Barhanin J, Lesage F, Guillemare E, Fink M, Lazdunski M, and Romey G (1996) K(V)LQT1
and IsK (MinK) Proteins Associate to Form the I(Ks) Cardiac Potassium Current. *Nature*
384:78-80.

Bosch RF, Gaspo R, Busch AE, Lang HJ, Li GR, and Nattel S (1998) Effects of the
Chromanol 293B, a Selective Blocker of the Slow, Component of the Delayed Rectifier K+
Current, on Repolarization in Human and Guinea Pig Ventricular Myocytes. *Cardiovasc Res*
38:441-450.

Bruhova I, and Zhorov BS (2005) KvAP-based model of the pore region of Shaker potassium
channel is consistent with cadmium- and ligand-binding experiments. *Biophys J* **89**:1020-
1029.

Bruhova I, and Zhorov BS (2007) Monte Carlo-energy minimization of correolide in the
Kv1.3 channel: Possible role of potassium ion in ligand-receptor interactions. *BMC Struct
Biol* **7**(1):5.

Decher N, Pirard B, Bundis F, Peukert S, Baringhaus KH, Busch AE, Steinmeyer K, and
Sanguinetti MC (2004) Molecular basis for Kv1.5 channel block: conservation of drug
binding sites among voltage-gated K+ channels. *J Biol Chem* **279**(1):394-400.

Doyle DA, Morais CJ, Pfuetzner RA, Kuo A, Gulbis JM, Cohen SL, Chait BT, and
MacKinnon R (1998) The Structure of the Potassium Channel: Molecular Basis of K+
Conduction and Selectivity. *Science* **280**:69-77.

Du LP, Li MY, Tsai KC, You QD, and Xia L (2005) Characterization of Binding Site of
Closed-State KCNQ1 Potassium Channel by Homology Modeling, Molecular Docking, and
Pharmacophore Identification. *Biochem Biophys Res Commun* **332**:677-687.

Gerlach U (2003) Blockers of the Slowly Delayed Rectifier Potassium IKs Channel: Potential
Antiarrhythmic Agents. *Curr Med Chem Cardiovasc Hematol Agents* **1**:243-252.

Gerlach U, Brendel J, Lang HJ, Paulus EF, Weidmann K, Bruggemann A, Busch AE,
Suessbrich H, Bleich M, and Greger R (2001) Synthesis and Activity of Novel and Selective
I(Ks)-Channel Blockers. *J Med Chem* **44**:3831-3837.

Hanner M, Green B, Gao YD, Schmalhofer WA, Matyskiela M, Durand DJ, Felix JP, Linde
AR, Bordallo C, Kaczorowski GJ, Kohler M, and Garcia M L (2001) Binding of Correolide to
the K(v)1.3 Potassium Channel: Characterization of the Binding Domain by Site-Directed
Mutagenesis. *Biochemistry* **40**:11687-11697.

Keating MT, and Sanguinetti MC (2001) Molecular and Cellular Mechanisms of Cardiac
Arrhythmias. *Cell* **104**:569-580.

Lazaridis T, and M. Karplus. (1999) Effective energy function for proteins in solution.
Proteins **35**:133-152.

Lerche C, Scherer CR, Seebohm G, Derst C, Wei AD, Busch AE, and Steinmeyer K (2000a)
Molecular Cloning and Functional Expression of KCNQ5, a Potassium Channel Subunit That
May Contribute to Neuronal M-Current Diversity. *J Biol Chem* **275**:22395-22400.

Lerche C, Seebohm G, Wagner CI, Scherer CR, Dehmelt L, Abitbol I, Gerlach U, Brendel J,
Attali B, and Busch AE (2000b) Molecular Impact of MinK on the Enantiospecific Block of
I(Ks) by Chromanols. *Br J Pharmacol* **131**:1503-1506.

Li Z, and Scheraga HA (1987) Monte Carlo-minimization approach to the multiple-minima problem in protein folding. *Proc Natl Acad Sci USA* **84**:6611-6615.

Long SB, Campbell EB, and MacKinnon R (2005) Crystal Structure of a Mammalian Voltage-Dependent Shaker Family K+ Channel. *Science* **309**:897-903.

Maljevic S, Lerche C, Seebohm G, Alekov AK, Busch AE, and Lerche H (2003) C-Terminal Interaction of KCNQ2 and KCNQ3 K+ Channels. *J Physiol* **548**:353-360.

Melman YF, Um SY, Krumerman A, Kagan A, and McDonald TV (2004) KCNE1 Binds to the KCNQ1 Pore to Regulate Potassium Channel Activity. *Neuron* **42**:927-937.

Mitcheson JS, Chen J, Lin M, Culberson C, and Sanguinetti MC (2000) A Structural Basis for Drug-Induced Long QT Syndrome. *Proc Natl Acad Sci USA* **97**:12329-12333.

Momany FA, McGuire RF, Burgess AW, and Scheraga HA (1975) Energy parameters in polypeptides. VII. Geometric parameters, partial atomic charges, nonbonded interactions, hydrogen bond interactions, and intrinsic torsional potentials of the naturally occurring amino acids. *J Phys Chem* **79**:2361-2381.

Roden DM (1993) Torsade De Pointes. *Clin Cardiol* **16**:683-686.

Roux B, and MacKinnon R (1999) The Cavity and Pore Helices in the KcsA K+ Channel: Electrostatic Stabilization of Monovalent Cations. *Science* **285**:100-102.

Sanguinetti MC (1992) Modulation of Potassium Channels by Antiarrhythmic and Antihypertensive Drugs. *Hypertension* **19**:228-236.

Sanguinetti MC, Chen J, Fernandez D, Kamiya K, Mitcheson J, and Sanchez-Chapula JA (2005) Physicochemical Basis for Binding and Voltage-Dependent Block of HERG Channels by Structurally Diverse Drugs. *Novartis Found Symp* **266**:159-166.

Sanguinetti MC, Curran ME, Zou A, Shen J, Spector PS, Atkinson DL, and Keating MT (1996) Coassembly of K(V)LQT1 and MinK (IsK) Proteins to Form Cardiac I(Ks) Potassium Channel. *Nature* **384**:80-83.

Sanguinetti MC, and Jurkiewicz NK (1991) Delayed Rectifier Outward K+ Current Is Composed of Two Currents in Guinea Pig Atrial Cells. *Am J Physiol* **260**:H393-H399.

Schmitt N, Schwarz M, Peretz A, Abitbol I, Attali B, and Pongs O (2000) A Recessive C-Terminal Jervell and Lange-Nielsen Mutation of the KCNQ1 Channel Impairs Subunit Assembly. *EMBO J* **19**:332-340.

Schreieck J, Wang Y, Gjini V, Korth M, Zrenner B, Schomig A, and Schmitt C (1997) Differential Effect of Beta-Adrenergic Stimulation on the Frequency-Dependent Electrophysiologic Actions of the New Class III Antiarrhythmics Dofetilide, Ambasilide, and Chromanol 293B. *J Cardiovasc Electrophysiol* **8**:1420-1430.

Schwake M, Jentsch TJ and Friedrich T (2003) A Carboxy-Terminal Domain Determines the Subunit Specificity of KCNQ K+ Channel Assembly. *EMBO Rep* **4**:76-81.

Seebohm G, Chen J, Strutz N, Culberson C, Lerche C, and Sanguinetti MC (2003a) Molecular Determinants of KCNQ1 Channel Block by a Benzodiazepine. *Mol Pharmacol* **64**:70-77.

Seebohm G, Lerche C, Pusch M, Steinmeyer K, Bruggemann A, and Busch AE (2001a) A Kinetic Study on the Stereospecific Inhibition of KCNQ1 and I(Ks) by the Chromanol 293B. *Br J Pharmacol* **134**:1647-1654.

Seebohm G, Pusch M, Chen J, and Sanguinetti MC (2003b) Pharmacological Activation of Normal and Arrhythmia-Associated Mutant KCNQ1 Potassium Channels. *Circ Res* **93**:941-947.

Seebohm G, Scherer CR, Busch AE, and Lerche C (2001b) Identification of Specific Pore Residues Mediating KCNQ1 Inactivation. A Novel Mechanism for Long QT Syndrome. *J Biol Chem* **276**:13600-13605.

Singh NA, Charlier C, Stauffer D, DuPont BR, Leach RJ, Melis R, Ronen GM, Bjerre I, Quattlebaum T, Murphy JV, McHarg ML, Gagnon D, Rosales TO, Peiffer A, Anderson VE, and Leppert M (1998) A Novel Potassium Channel Gene, KCNQ2, Is Mutated in an Inherited Epilepsy of Newborns. *Nat Genet* **18**:25-29.

Takumi T, Ohkubo H, and Nakanishi S (1988) Cloning of a Membrane Protein That Induces a Slow Voltage-Gated Potassium Current. *Science* **242**:1042-1045.

Tapper AR, and George AL, Jr (2000) MinK Subdomains That Mediate Modulation of and Association With KvLQT1. *J Gen Physiol* **116**:379-390.

Tikhonov DB, and Zhorov BS (2005) Sodium channel activators: model of binding inside the pore and a possible mechanism of action. *FEBS Lett* **579**:4207-4212.

Tristani-Firouzi M, and Sanguinetti MC (1998) Voltage-Dependent Inactivation of the Human K+ Channel KvLQT1 Is Eliminated by Association With Minimal K+ Channel (MinK) Subunits. *J Physiol* **510 (Pt 1)**:37-45.

Wang S-Y, Mitchell J, Tikhonov DB, Zhorov BS, and Wang GK (2006) How batrachotoxin modifies the sodium channel permeation pathway: computer modeling and site-directed mutagenesis. *Mol Pharmacol* **69**(3):788-95.

Wei AD, Butler A, and Salkoff L (2005) KCNQ-Like Potassium Channels in Caenorhabditis Elegans. Conserved Properties and Modulation. *J Biol Chem* **280**:21337-21345.

Weiner SJ, Kollmann PA, Case DA, Singh UC, Ghio C, Alagona, G, Profeta S, and Weiner P (1984) A new force field for molecular mechanical simulation of nucleic acids and proteins. *J Amer Chem Soc* **106**:765-784.

Yang IC, Scherz MW, Bahinski A, Bennett PB, and Murray KT (2000) Stereoselective Interactions of the Enantiomers of Chromanol 293B With Human Voltage-Gated Potassium Channels. *J Pharmacol Exp Ther* **294**:955-962.

Zhou Y, Morais-Cabral JH, Kaufman A, and MacKinnon R (2001) Chemistry of Ion Coordination and Hydration Revealed by a K+ Channel-Fab Complex at 2.0 A Resolution. *Nature* **414**:43-48.

Zhou Y, and MacKinnon R (2003) The occupancy of ions in the K+ selectivity filter: charge balance and coupling of ion binding to a protein conformational change underlie high conduction rates. *J Mol Biol* **333**:965-975.

Zhou M, and MacKinnon R (2004a) A Mutant KcsA K(+) Channel With Altered Conduction Properties and Selectivity Filter Ion Distribution. *J Mol Biol* **338**:839-846.

Zhou Y, and MacKinnon R (2004b) Ion Binding Affinity in the Cavity of the KcsA Potassium Channel. *Biochemistry* **43**:4978-4982.

Zhorov B S, and Ananthanarayanan VS (1996) Structural model of a synthetic Ca^{2+} channel with bound Ca^{2+} ions and dihydropyridine ligand. *Biophys J* **70**:22-37.

Zhorov BS, Folkman EV, and Ananthanarayanan VS (2001) Homology model of dihydropyridine receptor: implications for L-type Ca(2+) channel modulation by agonists and antagonists. *Biophys J* **393**:22-41.

Footnotes

Reprint requests to Guiscard Seebohm, Physiology I, University of Tuebingen, Gmelinstr. 5,

D-72076 Tuebingen, Germany, Tel.: +49 7071-29-78264, Fax.: +49 7071-29-3073, email:

guiscard.seebohm@gmx.de

Legends for figures

Figure 1

Different 293B sensitivity of KCNQ channels

A-H, Effect of 293B at indicated concentrations (in µM) on different KCNQ channel currents elicited during voltage steps from –80 mV to +40 mV in oocytes (n = 3-5). Horizontal scale bars represent 0.5 sec.

Figure 2

Chimeras identifying important regions for chromanol 293B binding

A, Models showing the typical backbone of a voltage-dependent potassium channel subunit with intracellular C- and N-Terminus and six transmembrane domains. Black and grey lines indicate KCNQ1 and KCNQ2 sequences, respectively. *B*, Alignment of KCNQ channel protein sequences of H5 pore loop and S6 transmembrane regions. Differences in amino acids are marked by arrows. Positions of mutations with neutral effects on 293B affinity are marked by white arrows and those with mild and strong effects with grey and black arrows, respectively.

Figure 3

Point mutations decrease chromanol sensitivity in KCNQ1

A-G, Currents of indicated KCNQ1 mutants recorded in absence or presence of KCNE1 before and after treatment with chromanol 293B. Currents were recorded in oocytes (n = 3-8) during voltage steps from –80 mV to +40 mV. KCNQ1 T312S/KCNE1 mutant currents could not be differentiated from endogenous *Xenopus* KCNQ1/KCNE1 currents when injected with KCNE1 only and are not shown. Horizontal scale bars represent 1 sec, vertical scale bars 1µA. *H,* Bars represent mean IC_{50} values of chromanol block (n = 3-8). The exact IC_{50} values are summarized in Table 3. Due to solubility the maximal used concentration of chromanol

293B was 100 µM. IC$_{50}$ values above 100 µM were calculated assuming a Hill-coefficient of 1.

Figure 4

Introduction of Chromanol 293B sensitivity into KCNQ2

Introduction of two residues of the 293B binding site of KCNQ1 is sufficient to confer novel 293B-sensitivity into KCNQ2 (KCNQ2(L272V/V302I)), while the reverse exchange disrupts 293B-sensitivity of KCNQ1 (KCNQ1(V307L/I337V)). Black and grey lines indicate KCNQ1 and KCNQ2 sequences, respectively.

Figure 5

Docking of a 293B molecule within the cavity of the homology models of the KCNQ1 channel

A − F, Open channel model of KCNQ1 derived from the Kv1.2 X-ray structure. Side views (*A* and *C*), and top views (*B* and *D*) of random orientations of 293B inside the channel. *A* and *B,* only 200 of 20,000 positions are shown. *C* and *D*, superposition of the five most energetically favorable binding modes of 293B within the channel. *E* and *F*, typical low-energy binding mode of a 293B molecule within the cavity of the open channel. Residues I337 and F340 are shown as gray sticks. *G* and *H*, typical low-energy binding mode of a 293B molecule within the cavity of the closed channel derived from the KcsA X-ray structure. For clarity, hydrogen atoms are not shown. Only inner and outer helices of 2 subunits are shown in *E* and *G*. *E* and *G* contain close-up views. Potassium ions (in yellow) and water molecules (CPK-code) are shown in space fill. The inner S5 helix is represented in purple, the pore helix, selectivity filter and linkers are coloured green and the outer S6 helices are gray. *I*, structure of 293B molecule (trans-6-cyano-4-(N-ethylsulfonyl-N-methylamino)-3-hydroxy-2,2-dimethyl-chroman). Left figure: introduction of large substituents at the sulfonyl group (blue) at the site

depicted in red were reported to increase IC_{50} values, whereas large hydrophobic substituents

at C6 of the chroman (purple) decrease the IC_{50}. CPK-coloured ball and stick model of 293B

(middle). To the right 293B is depicted by surface rendered representations. The colouring

indicates the calculated electrostatic potentials $\pm$ energy values (scale bar as indicated: +0.05

and -0.05 iso-valued surfaces). The two oxygens of the sulfonyl group and the one attached to

the chroman ring (at C3) represent a strong negative charge (red areas marked by * in the

right hand figure), which may be the molecular basis for a strong electrostatic interaction with

the positively charged potassium ion in the lower selectivity filter.

Tables

Table 1. 293B-Sensitivity of KCNQ channels

IC_{50} *values are expressed as mean $\pm$ SEM, n indicates number of experiments.*

Channel	***IC_{50} or inhibition at 100 µM of 293B**
KCNQ1	*26.9 $\pm$ 0.8 µM (n = 5)
KCNQ1/KCNE1	*6.9 $\pm$ 0.5 µM (n = 5)
KCNQ2	~5 % (n = 3)
KCNQ3	~5 % (n = 3)
KCNQ4	~10 % (n = 5)
KCNQ5	~40 % (n = 3)
KQT1	*16.2 $\pm$ 1.3 µM (n = 3)
KCNQ2/KCNQ3	~5 % (n = 3)
KCNQ3/KCNQ5	~25 % (n = 3)

31

Table 2. 293B-Sensitivity of WT and chimeric KCNQ1/KCNQ2 channels

IC_{50} values are expressed as mean ± SEM, n indicates number of experiments.

Channel	*IC_{50} or inhibition at 100 μM of 293B
KCNQ1	*26.9 ± 0.8 μM (n = 5)
KCNQ2	~5 % (n = 3)
Q1S5S6Q2	~20 % (n = 3)
Q2S5S6Q1	*56.2 ± 1.6 μM (n = 6)
Q1S5Q2	*38,7 ± 2,9 μM (n = 4)
Q1S5linkerQ2	*32.5 ± 2.1 μM (n = 3)
Q1S5H5Q2	~35 % (n = 3)
Q1H5S6Q2	~10 % (n = 3)

Table 3. 293B-Sensitivity of mutant KCNQ1 channels

IC_{50} values are expressed as mean ± SEM, n indicates number of experiments.

Mutation in KCNQ1	***IC_{50} or inhibition at 100 μM of 293B on KCNQ1**	***IC_{50} or inhibition at 100 μM of 293B on KCNQ1/KCNE1 (I_{Ks})**
KCNQ1 wt	*26.9 ± 0.8 μM (n = 5)	*6.9 ± 0.5 μM (n = 5)
V307L	48,7 ± 3, 2% (n = 4)	49,9 ± 2, 2% (n = 4)
V310L	*70.5 ± 2.1 μM (n = 3)	*30.5 ± 1.1 μM (n = 3)
T311S	*30.1 ± 1.7 μM (n = 3)	*7.2 ± 0.7 μM (n = 3)
T311A	no functional expression	not tested
T312S	~10 % (n = 4)	not tested
K326R/T327L	*29,5 ± 1,1 μM (n = 3)	not tested
S330A/C331T	*32,4 ± 2,0 μM (n = 3)	not tested
F335Y	~50 % (n = 3)	*9.1 ± 2.5 μM (n = 3)
A336T	~40 % (n = 3)	~50 % (n = 3)
I337V	~35 % (n = 4)	~39 % (n = 4)
S338T	~40 % (n = 4)	*10.2 ± 3.7 μM (n = 4)
F339Y	~40 % (n = 3)	*20.2 ± 1.7 μM (n = 3)
F340I	~20 % (n = 3)	not tested
F340Y	~10 % (n = 4)	~30 % (n = 4)

Table 4. Sequence alignment of K⁺ channels

Outer helix [†]							
KcsA	14	KLLLGRHGSA	LHWRAAGAAT	VLLVIVLLAG	SYLAVLAERG	APGA	57
Kv1.2	313	GLQILGQTLK	ASMRELGLLI	FFLFIGVILF	SSAVYFAEAG	SENS	356
KCNQ1	247	TWRLLGSVVF	IHRQELITTL	YIGFLGLIFS	SYFVYLAEKD	AVNE	290

P-loop/H5					
KcsA	58	QLITYPRALW	WSVETATTVG	YGDLYPVT	85
Kv1.2	357	FFPSIPDAFW	WAVVSMTTVG	YGDMVPTT	384
KCNQ1	295	EFGSYADALW	WGVVTVT**T**IG	YGDKVPQT	422

Inner helix [*]					
KcsA	86	LWGRLVAVVV	MVAGITSFGL	VTAALATWFV	GREQ	120
Kv1.2	385	IGGKIVGSLC	AIAGVLTIAL	PVPVIVSNFN	YFYH	418
KCNQ1	423	WVGKTIASCF	SVFA**I**SF**F**AL	PAGILGSGFA	LKVQ	456

[†] The outer helices were aligned according to Bruhova and Zhorov (2005). 293B-sensing

residues in the pore loop and inner helices of KCNQ1 are bold and underlined.

Table 5. Energy components (kcal/mol) of the most energetically favourable complexes of
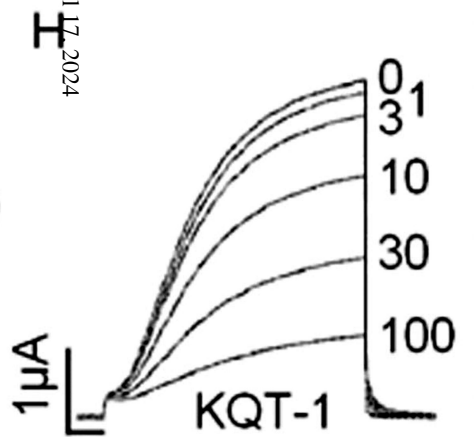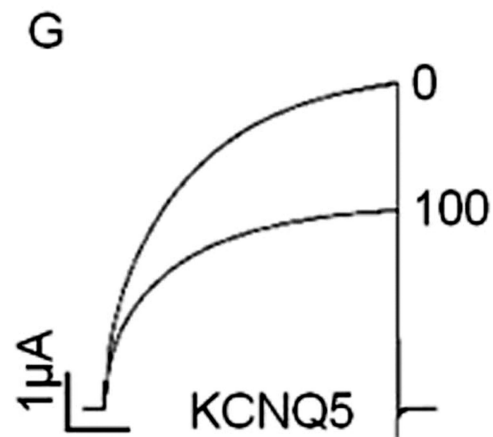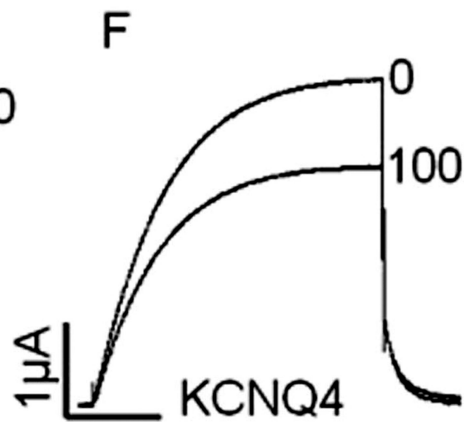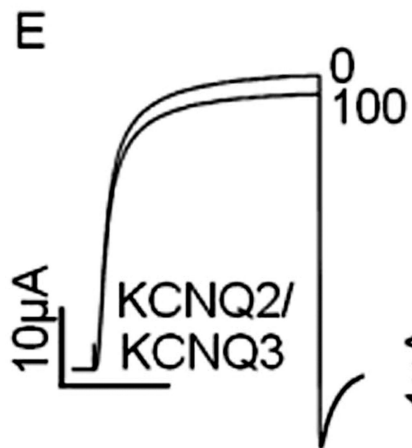
chromanol inside KCNQ1

Energy component	Open channel	Closed channel
Ligand-receptor components		
van der Waals	−5.1	−13.8
Electrostatic	−26.7	−30.4
Solvation	12.2	14.8
Ligand components		
Intra-ligand nonbonded [†]	−9.6	0.6
Ligand strain [‡]	9.0	16.2
Total	−20.2	−12.6
Major contributors to ligand binding energy [#]		
K^+ in position 4	−14.1	−13.3
H_2O in position 3	−1.4	−2.3
T311	−0.8	−4.9
T312	−1.9 (−2.2/1.9)	−1.8 (−4.7/4.6)
I337	−2.4	−3.6
F340	−0.8	−5.8

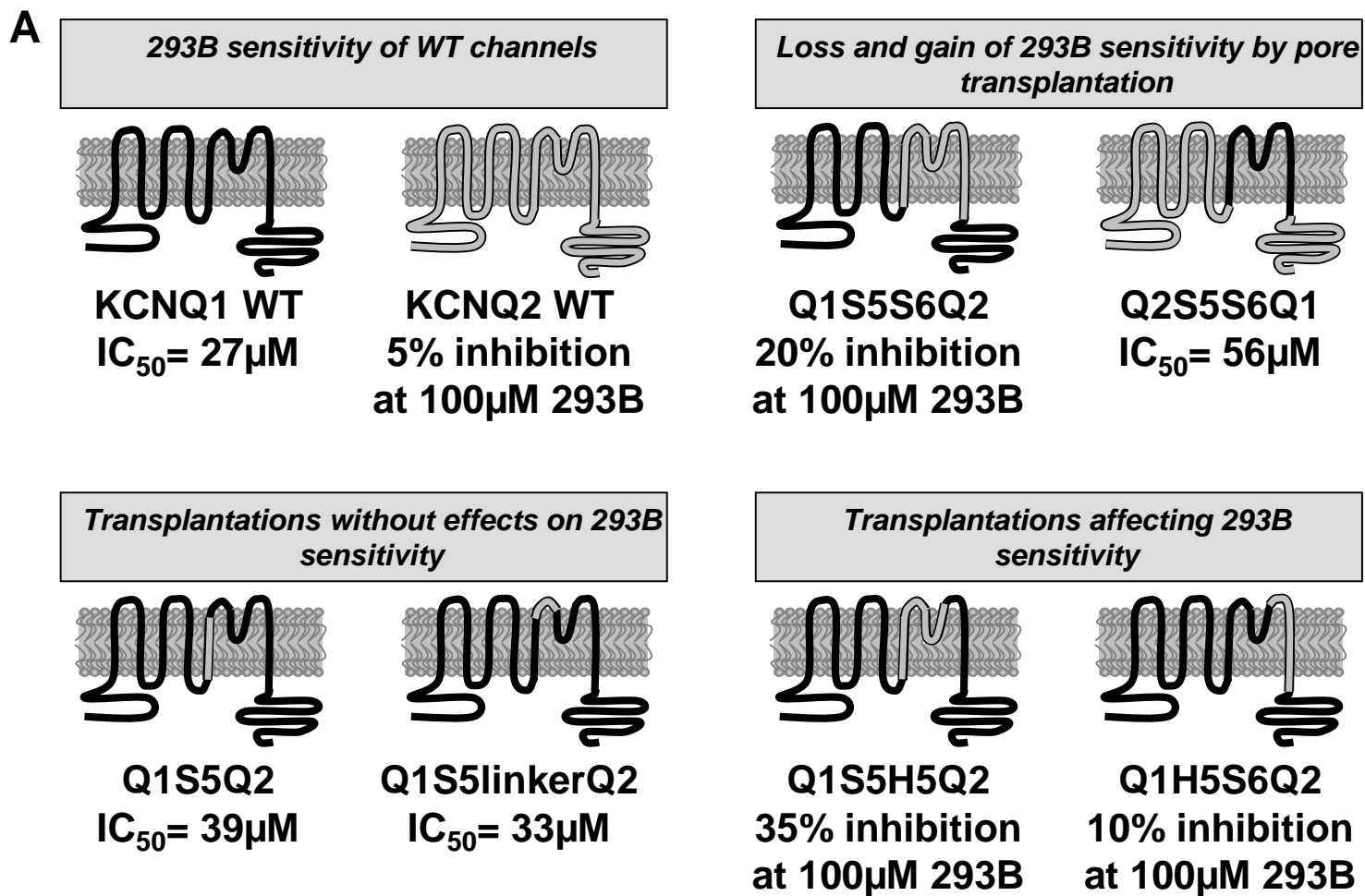[†] The sum of atom-atom interactions of the ligand

[‡] The sum of energy of deformation of bond angles plus torsional energy of the ligand.

The energy contribution of a residue to ligand binding is summed over four subunits.The

first number is the sum of contributions from the four domains. The values in brackets show

the minimal and the maximal contributions from individual domains.
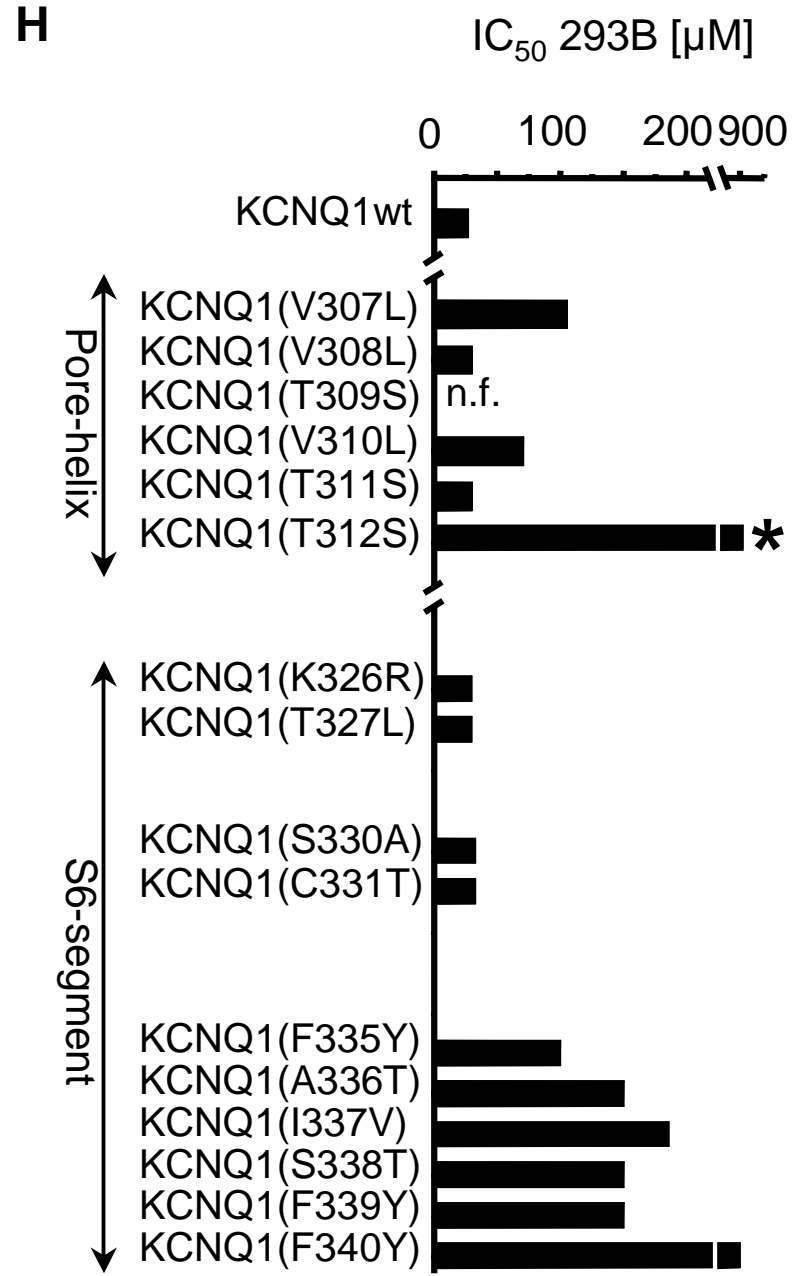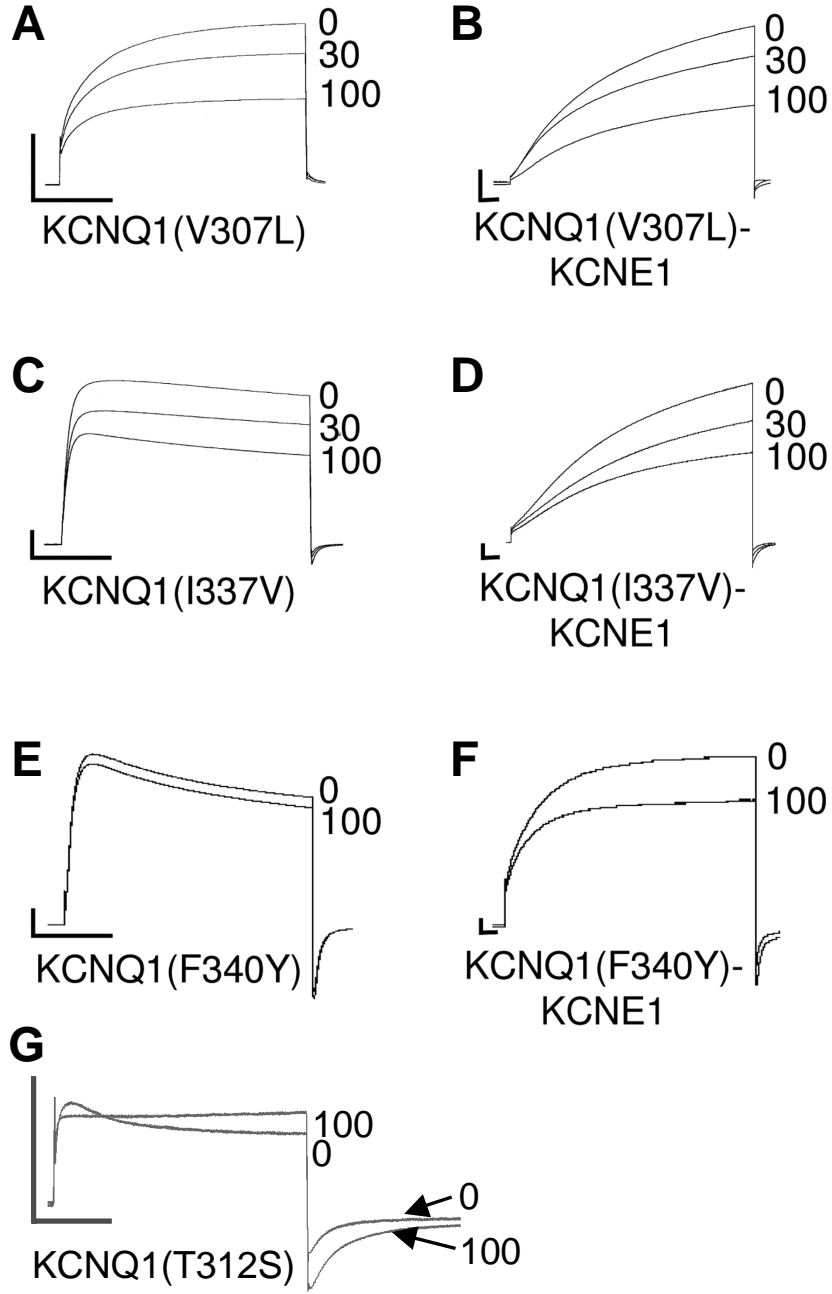
1

2

A

293B sensitivity of WT channels

KCNQ1 WT
$IC_{50}= 27\mu M$

KCNQ2 WT
5% inhibition
at 100µM 293B

Loss and gain of 293B sensitivity by pore transplantation

Q1S5S6Q2
20% inhibition
at 100µM 293B

Q2S5S6Q1
$IC_{50}= 56\mu M$

Transplantations without effects on 293B sensitivity

Q1S5Q2
$IC_{50}= 39\mu M$

Q1S5linkerQ2
$IC_{50}= 33\mu M$

Transplantations affecting 293B sensitivity

Q1S5H5Q2
35% inhibition
at 100µM 293B

Q1H5S6Q2
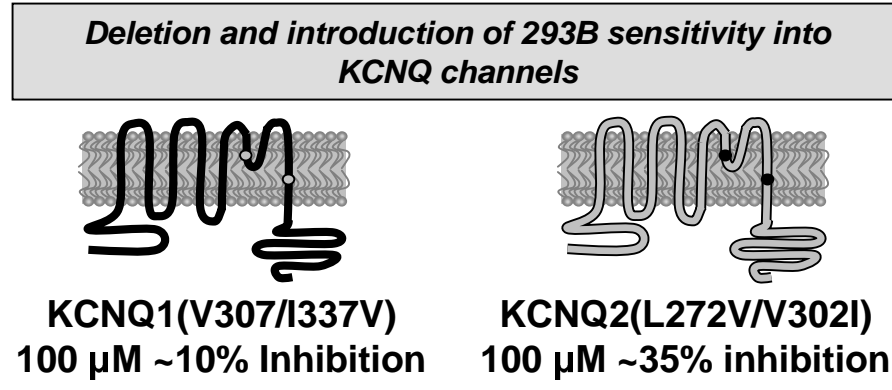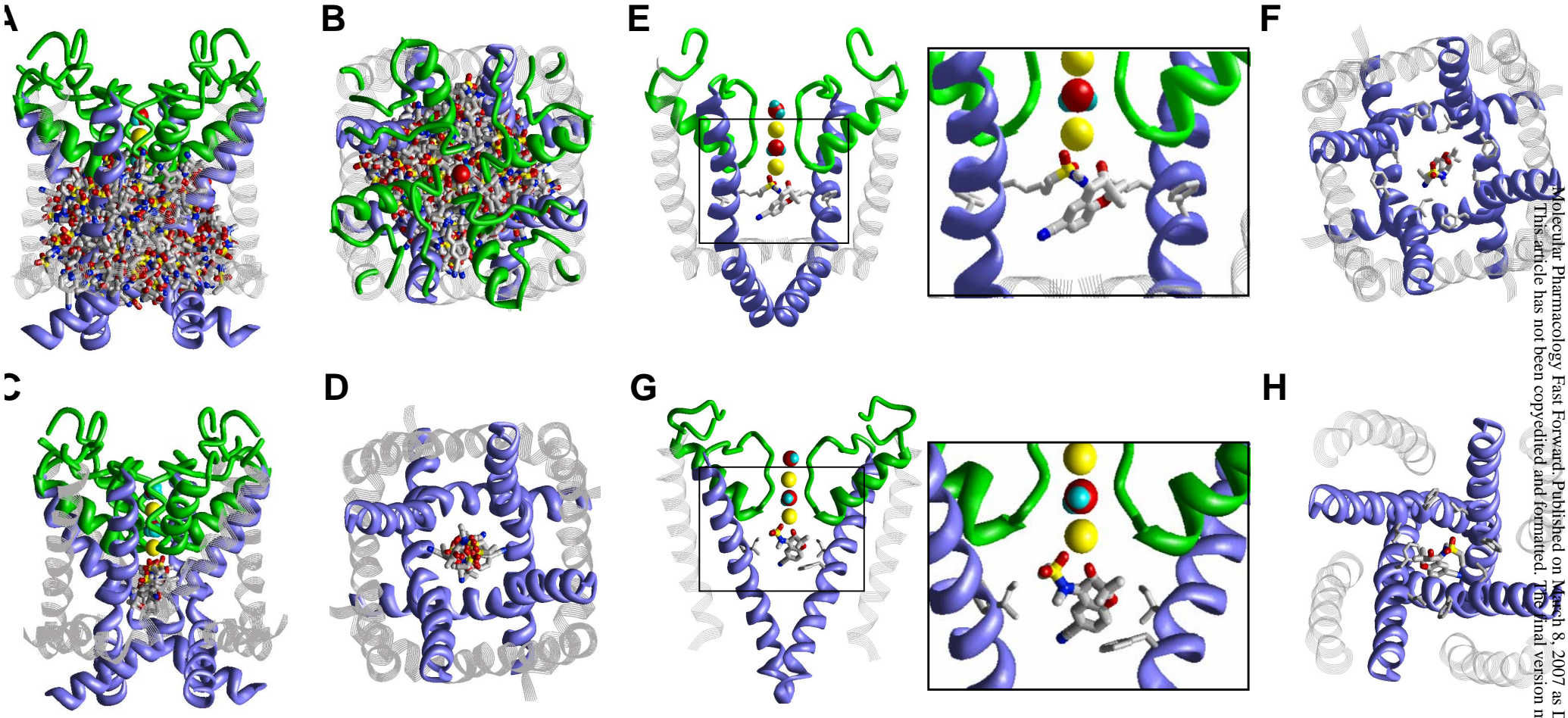10% inhibition
at 100µM 293B

B

```
KCNQ1   GVVTVTTIGYGDKVPQTWVGKTIASCFSVFAISFFALPAGILGS   349
KCNQ2   GLITLTTIGYGDKYPQTWNGRLLAATFTLIGVSFFALPAGILGS   314
KCNQ3   GLITLATIGYGDKTPKTWEGRLIAATFSLIGVSFFALPAGILGS   353
KCNQ4   GTITLTTIGYGDKTPETWLGRVLAAGFALLGISFFALPAGILGS   320
KCNQ5   GTITLTTIGYGDKTPLTWLGRLLSAGFALLGISFFALPAGILGS   348
KQT1    GVITLSTVGYGDKTPETWPGKIIAAFCALLGISFFALPAGILGS   334
```

3

A KCNQ1(V307L)
0 / 30 / 100

B KCNQ1(V307L)-KCNE1
0 / 30 / 100

C KCNQ1(I337V)
0 / 30 / 100

D KCNQ1(I337V)-KCNE1
0 / 30 / 100

E KCNQ1(F340Y)
0 / 100

F KCNQ1(F340Y)-KCNE1
0 / 100

G KCNQ1(T312S)
100 / 0 / 0 / 100

H IC_{50} 293B [µM]

0   100   200 900

KCNQ1wt

Pore-helix
KCNQ1(V307L)
KCNQ1(V308L)
KCNQ1(T309S) n.f.
KCNQ1(V310L)
KCNQ1(T311S)
KCNQ1(T312S) *

S6-segment
KCNQ1(K326R)
KCNQ1(T327L)
KCNQ1(S330A)
KCNQ1(C331T)
KCNQ1(F335Y)
KCNQ1(A336T)
KCNQ1(I337V)
KCNQ1(S338T)
KCNQ1(F339Y)
KCNQ1(F340Y)

Deletion and introduction of 293B sensitivity into KCNQ channels

KCNQ1(V307/I337V)
100 µM ~10% Inhibition

KCNQ2(L272V/V302I)
100 µM ~35% inhibition

I Chromanol 293B